Comparative Conformational Dynamics of Supercoiled Plasmids and Linear DNA during Capillary Electrophoresis

Jeffrey J. Schwinefus,[†] Richard W. Hammond,[†,||] Hidehiro Oana,[‡] Shau-Chun Wang,[†] Olivia De Carmejane,[†] Jeffrey Bonadio,[§] and Michael D. Morris*[,†]

Department of Chemistry, University of Michigan, Ann Arbor, Michigan 48109, Department of Physics, Kyoto University, Kyoto, 606-8502, Japan, and Selective Genetics, Inc., San Diego, California 92121

Received January 29, 1999; Revised Manuscript Received May 14, 1999

ABSTRACT: The electrophoretic migration of 40 and 90 kbp supercoiled (sc) double-stranded (ds) plasmid DNA in dilute and entangled solutions of linear hydroxyethyl cellulose (HEC, $M_n = 438\,800$) was visualized by video fluorescence microscopy at 60−222 frames/s. The sc-DNA molecules migrated as elastic rods with stretch−contraction cycles directed along the electric field axis. The elastic rod electrophoretic behavior of sc-DNA is completely different from the familiar random coil electrophoretic dynamics of linear ds-DNA. Extension−contraction cycles were more periodic for sc-DNA than for linear ds-DNA. The consequences of the different sc-DNA and linear ds-DNA electrophoretic dynamics on mobility dispersion are discussed.

Introduction

Visualization of long (50 000 base pair, 50 kbp, or longer) linear double-stranded (ds) DNA has been widely employed to develop models of biopolymer electrophoresis.[1−8] It has been assumed that the observed dynamics are generally applicable. But, while longer polyelectrolytes behave as random coils, shorter ones behave more like elastic or rigid rods.[9]

We present here the first direct visual comparison of elastic rod and random coil electrophoretic dynamics. Direct visualization, which has proven so useful in understanding behavior of random coils, has not been attempted for rods. This gap in our understanding is doubly surprising because linear ds-DNA has generally served as a model for the behavior of long polymers,[10−13] and it has been surmised that supercoiled (sc) plasmids may behave as rods.[14,15]

Plasmids are circular, ds-DNA molecules that replicate in bacteria such as *Escherichia coli*.[16] Prototypical plasmid cloning and expression vectors usually are less than 10 kbp, contain a gene for antibiotic resistance, and typically generate many tens or hundreds of copies within each host cell. Unique restriction endonuclease cleavage sites exist within plasmid vectors that allow for the assembly of recombinant DNA molecules. This technology is a foundation for both molecular biology and biotechnology. Purified ds-plasmid DNA molecules assume a supercoiled conformation.[17] Supercoiling has been studied extensively using theoretical simulations,[18,19] scanning force microscopy,[20,21] and light scattering experiments.[14,15] Recent dynamic light scattering studies[14] suggest that in solution 3.8 kbp plasmids behave as stiff interwound coils that fluctuate among different conformations, approximating rodlike behavior.

Dilute linear polymer solutions have enabled rapid separation of linear ds-DNA fragments.[22,23] Recently our group reported for the first time the high mobility dispersion and anomalously broad bands of capillary electropherograms observed for sc-plasmid DNA compared to linear ds-DNA over the same size range in dilute hydroxyethyl cellulose (HEC).[24,25] The broad Gaussian bands were due to a thermal distribution of topoisomers or plasmids with the same chain length that differ in the number of supercoils.[17] Resolution of individual topoisomers is possible on agarose gels after supercoil unwinding.[26−28] Liquid crystal media[29] and dilute hydroxypropylmethyl cellulose (HPMC) solutions[30] have also yielded at least partial resolution of topoisomers without unwinding.

Our own capillary electrophoresis (CE) studies suggest that the field-driven dynamics of sc-DNA in dilute linear polymer solutions are quite different from the electrophoretic dynamics of linear ds-DNA fragments.[24,25] The plasmid mobilities were interpreted as consequences of plasmid migration as elastic rods using chain length scaling arguments, supplemented with brief visualization studies. Supercoiled plasmid mobility and linear ds-DNA mobility scale similarly with radius of gyration, R_g, assuming that the sc-DNA radius of gyration scales as M, the number of base pairs, as expected for an elastic rod,[9] and that linear DNA R_g scales with $M^{1/2}$, as appropriate for a wormlike chain.[9]

Smith and Bendich[31] have used 66 kbp plasmids trapped in agarose gels to measure charge density and persistence length while Song and Maestre[3] have measured the electrophoretic mobility of pBR322 plasmids. However, to our knowledge, the electrophoretic migration dynamics of sc-DNA have not been studied before. The electrophoresis results suggest that sc-DNA may serve as visualization models for dynamics of solutions of rodlike polymers.

Prompted by these unusual findings, we have examined the electrophoretic dynamics of supercoiled 40 and 90 kbp ds-plasmid DNA and linear λ phage ds-DNA (48.5 kbp) by high-speed fluorescence video microscopy. We have quantified the electrophoretic motions of both supercoiled and linear ds-DNA. The ramifications of the

* To whom correspondence should be addressed.
[†] University of Michigan.
[‡] Kyoto University.
[§] Selective Genetics, Inc.
[||] Current address: CuraGen, Corp., Branford, CT 06405.

10.1021/ma990129x CCC: $18.00
Published on Web 06/25/1999

completely different migration mechanisms of these two forms of DNA are discussed.

Experimental Section

Materials and Methods. Hydroxyethyl cellulose (HEC, M_n=438 800, Aqualon) was prepared as 0.008, 0.05, or 0.16% w/w solutions in 1X TBE (89 mM Tris, 89 mM boric acid, 2 mM EDTA). The concentrations of HEC used in this study bracket the entanglement limit of 0.09% w/w.[22] To reduce photobleaching, 2-mercaptoethanol (4% w/w) was added. Solutions were stirred for 24 h to ensure complete dissolution of the linear polymer.

Supercoiled 40 and 90 kbp plasmids (Research Genetics, Inc., Huntsville, AL) and linear λ phage ds-DNA (New England Biolabs, 48.5 kbp) were intercalated with POPO-3 (Molecular Probes, Eugene, OR) in 1X TBE prior to visualization. DNA concentrations in the electrophoresis medium were less than 0.04 ng/μL and were sufficiently low to prevent aggregation.[32] Supercoiled DNA images were obtained in 0.05% and 0.16% HEC. Linear DNA was imaged in 0.008% and 0.05% HEC. Imaging solutions contained approximately five base pairs per dye molecule.

The electrophoresis chamber consisted of two coverslips coated with polyacrylamide to prevent electroosmosis.[33] Ten microliters of sample were placed between the coverslips, and the coverslips were mounted between platinum electrodes spaced 2.5 cm apart on a glass slide. The spaces between coverslips and electrodes were filled with a 1% HEC solution to provide an electrical connection.

Instrumentation. An Olympus BH-2 infinity corrected microscope was the foundation of the microscopy system. Epi-illumination was with 70 mW or less 532 nm laser light passed through an optical fiber and a 50×/1.0 water immersion objective (Leitz, Rockleigh, NJ). The optical fiber was mechanically vibrated at 100−1,000 Hz to break up laser coherence. Data were collected with a progressive scan video camera (Pulnix, model TM-6701AN, Sunnyvale, CA) operated in the full frame (60 frames/s), 200 line (130 frames/s), or 100 line (222 frames/s) mode and a 60 MHz frame grabber (PDI, model IMAXX/PCI MM, Redmond, WA). The video camera was mounted on a lens-coupled image intensifier (Videoscope, Sterling, VA). Electrophoresis voltages were provided from a computer controlled high voltage amplifier (Trek, Medina, NY). A dc electric field of 100 V/cm was used for all studies.

Image Analysis. IPLab (Signal Analytics Corp., Viennna, VA) was used for image analysis. Image processing consisted of median filtering, dilation and center-of-mass measurement. Analysis of the electrophoretic behavior of sc-DNA and ds-linear DNA used the ellipsoidal model of Oana and co-workers.[8] The center of mass velocity (V_{cm}) and extension parallel (R_l) and perpendicular (R_s) to the electric field were used to quantify DNA migration dynamics. Specifically, R_l and R_s define one-fourth of the major and minor axes, respectively, of an ellipse defining the DNA molecule. A Savitsky−Golay derivative with a time increment of 1 frame was used to calculate the center of mass velocity.[34] R_l and R_s data were not smoothed.

To characterize the periodicity of DNA migration dynamics during electrophoresis we used the autocorrelation function[8] defined by eq 1. A *C* algorithm[35] was used to calculate

$$A_{yy}(\tau) = \frac{\int (y(t+\tau) - \bar{y})(y(t) - \bar{y})\, dt}{\int (y(t) - \bar{y})^2\, dt} \qquad (1)$$

the autocorrelation function for a function $y(t)$ and its time average $\bar{y}$.

Analysis of the average R_l peak shape follows that of Oana et al.[8] Peaks in the R_l data that were greater than the time average of R_l plus one standard deviation were chosen for the analysis. Generally, 15−20 peaks in R_l were chosen for analysis. Maxima were set to a time t_m. The chosen R_l peaks were then averaged, normalized by the average maximum, $\bar{R}_{l_{max}}$ and plotted vs $t - t_m$.

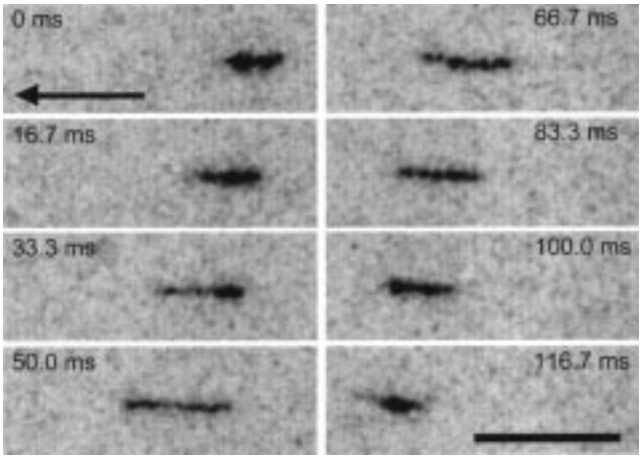

Figure 1. Electrophoretic migration of a 90 kbp sc-DNA molecule (stained with POPO-3) in a loosely entangled polymer solution (0.16% HEC, M_n = 438 800; 1X TBE) at 100 V/cm. The arrow indicates the direction of migration. Successive frames were taken at 17 ms intervals. Scale bar: 10 μm.

Results

Electrophoresis Dynamics. Using 60−222 frames/s, we could follow sc-DNA and linear DNA migration through unentangled HEC and entangled HEC in the absence of sucrose or other viscosity modifiers. The electric field migration patterns of the 40 and 90 kbp plasmids are completely different from any ever observed for linear ds-DNA.[1−8] Because the rotational correlation times of plasmids are shorter than our frame time, under field-free conditions, only the time-averaged spherical or slightly ellipsoidal unresolved shapes of plasmids could be seen at light microscope resolution. Details of supercoiling were not observable. Brownian motion was easily visible in both entangled and dilute HEC solutions. In the absence of HEC, the plasmids migrated as spheres even at 100 V/cm. But in the presence of HEC, the migration dynamics are best described as those of an elastic rod. The typical U or J shapes seen for linear DNA in media ranging from agarose gels[1,2,8] to dilute polymer solutions[4−7] were rarely observed during sc-DNA migration.

The tiled images (consecutive frames, 60 frames/s) of Figure 1 show a 90 kbp plasmid migrating through semidilute (0.16%) HEC at 100 V/cm. When the voltage is first applied, the sc-DNA molecule migrates briefly as a sphere until extension begins. The molecule then moves with a regular stretch-contraction cycle, repeated approximately every 150 ms. The maximum extension is short, rarely exceeding 6−7 μm. The images are representative of steady-state migration behavior. Motion of this type would be expected of a stiff spring with a weight on its trailing end dragged along a high-friction surface. The behavior of the 40 kbp sc-plasmid in semidilute solution is similar, but less detail is observable at light microscopic resolution.

Upon collision with HEC, the majority of the sc-DNA mass remains at the rear of the molecule, while a slender section extends forward (Figure 1, 16.7 ms). As the molecule's extension increases, mass is transferred to the leading head until a dumbbell shape forms. As the cycle continues, mass continues to move toward the front, until the stretched molecule suddenly collapses. Collapse to a ball is not complete, however, before a new

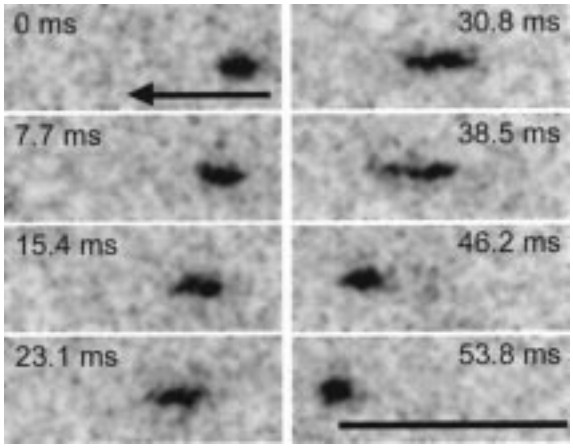

Figure 2. Time sequence of 40 kbp sc-DNA electrophoretic migration in 0.05% HEC (M_n = 438 800), 1X TBE at 100 V/cm. The arrow indicates the direction of migration. Consecutive frames from a 130 frames/s sequence. Scale bar: 10 μm.

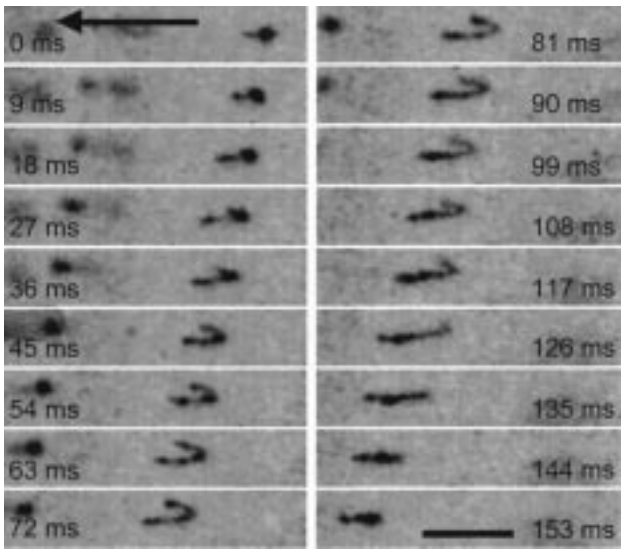

Figure 3. Electrophoretic migration of a linear λ (48.5 kbp) ds-DNA molecule in a dilute polymer solution (0.05% HEC, M_n = 438 800; 1X TBE) at 100 V/cm. The arrow pointing left indicates the direction of migration. Every other frame was taken from a 222 frames/s sequence (9 ms between frames). Frames were not averaged. Scale bar: 10 μm.

extension-contraction cycle begins. This elastic rod behavior was observed for both 40 kbp and 90 kbp sc-plasmids in 0.05% and 0.16% HEC. Figure 2 shows a 40 kbp sc-DNA molecule migrating in 0.05% HEC, 1X TBE with an electric field of 100 V/cm. The stretch−contraction cycle for 40 kbp sc-DNA is shorter than that observed for 90 kbp sc-DNA in both 0.16% HEC and 0.05% HEC. As in the semidilute case, for the shorter plasmid more extension−contraction cycles are observable across the field of view, but details of the dynamics are more easily observed for the longer plasmid.

Migration of linear ds-DNA in an I-shape conformation has been observed in concentrated (6−9%) linear polyacrylamide.[36] However, this migration behavior is due to constraints from neighboring polymer molecules and is unlike the elastic rod dynamics exhibited by sc-DNA.

Figure 3 illustrates the migration of linear λ (48.5 kbp) ds-DNA in 0.05% HEC with an electric field of 100 V/cm. In general, linear DNA migrates as a random coil before collision with HEC. Upon collision, the molecule

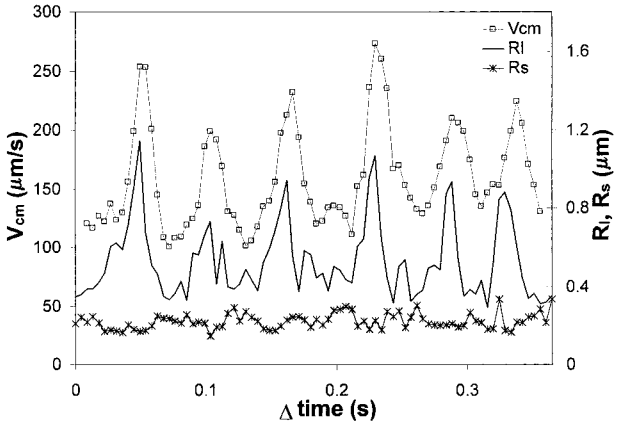

Figure 4. Time evolution of V_{cm}, R_l, and R_s for a 40 kbp sc-DNA molecule in 0.05% HEC, 1X TBE, 100 V/cm.

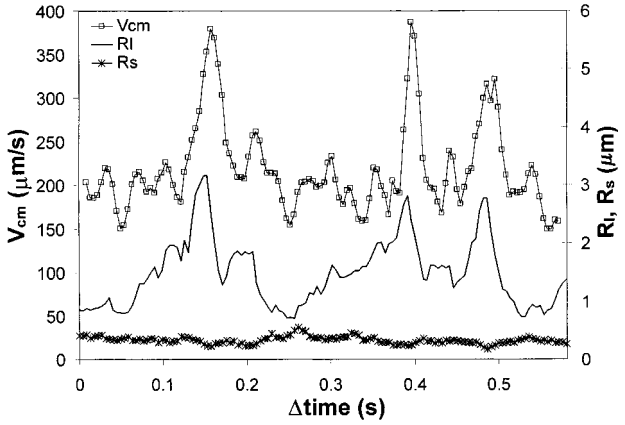

Figure 5. Time evolution of V_{cm}, R_l, and R_s for a linear λ (48.5 kbp) ds-DNA molecule in 0.05% HEC, 1X TBE, 100 V/cm.

extends both arms forming an apex in a U or J shape. Eventually, one arm grows at the expense of the other until the molecule slips off the obstruction and collapses back into the random coil. This is the widely observed motion of linear ds-DNA.[1−8]

We focus our quantitative analysis on the 40 kbp sc-DNA because of the greater number of oscillation cycles across the field of view. Figure 4 shows the evolution of the center of mass velocity, V_{cm}, of a 40 kbp sc-DNA molecule in 0.05% HEC at 100 V/cm through six cycles. The radii of extension along the major axis (parallel to the field), R_l and along the minor axis, R_s, are also shown. Maxima in V_{cm} are due to the entropic restoring force of the stretched molecule. V_{cm} and R_l oscillate at the same frequency. V_{cm} lags R_l slightly, which is consistent with a restoring force pulling the molecule back into a tight sphere. At the resolution of these experiments R_s does not change dramatically.

Figure 5 shows the time evolution of V_{cm} and R_l for linear λ ds-DNA under the same conditions as in Figure 4. The average V_{cm} is greater for the linear DNA than for the sc-DNA of similar size in base pairs, and so are the V_{cm} excursions. The V_{cm} oscillation period of λ DNA is longer than that of the 40 kbp sc-DNA, indicating longer entanglement times with HEC. Oscillations in linear ds-DNA V_{cm}, resulting from DNA/polymer entanglement and subsequent release, have been observed previously.[4,5,7,8] The implications for electrophoretic bandwidths have been discussed.[37−40]

The migration of the 40 kbp sc-DNA in entangled 0.16% HEC at 100 V/cm is essentially the same as in

the 0.05% unentangled solution. The time average extension of the 40 kbp sc-DNA in 0.16% HEC (1.5 ± 0.2 μm) is slightly larger than in 0.05% HEC (1.4 ± 0.1 μm). The average center of mass velocity of 93 ± 10 μm/s in 0.16% HEC is smaller than in unentangled 0.05% HEC (131 ± 25 μm/s) because of the greater number of entangling collisions, as well as the increased bulk solution viscosity. The magnitude of V_{cm} fluctuations are comparable to those in the unentangled solution, but the oscillations are more regular.

Migration of linear ds-DNA in 0.008% HEC at 100 V/cm proceeds with less extension than in 0.05% HEC. The time average extension of 48.5 kbp linear DNA in 0.008% and 0.05% HEC was determined to be 4.1 ± 0.5 and 4.5 ± 0.6 μm, respectively. Apexes of the U and J shapes are much narrower than in 0.05% HEC. Oscillations of V_{cm} are less regular than those of sc-DNA under similar conditions. The linear λ ds-DNA time average V_{cm} was determined to be 305 ± 81 μm/s in 0.008% HEC and 197 ± 73 μm/s in 0.05% HEC. The center of mass velocity of 48.5 kbp linear DNA is significantly larger than that of 40 kbp sc-DNA in 0.05% HEC. The behavior is qualitatively similar and quantitatively quite different at different HEC concentrations.

Using the approximations of Shi and co-workers[4] and the force-extension data of Strick et al.,[41] we estimate the extension of a 40 kbp sc-DNA molecule caused by entanglement of a single HEC molecule in 0.05% HEC to be 0.9 μm if the relative supercoiling is −0.031, and 3.3 μm if the relative supercoiling is −0.01 (average velocity = 131 μm/s, solution viscosity = 1.54 cP). In 0.16% HEC, entanglement with a single HEC molecule should extend the 40 kbp sc-DNA 0.7 μm if the relative supercoiling is −0.102, 2.2 μm if the relative supercoiling is −0.031, and 4.6 μm if the relative supercoiling is −0.01 (average velocity = 93 μm/s, solution viscosity = 4.93 cP). This range of relative supercoiling brackets values typical for purified plasmid DNA produced by standard fermentation methods.[17] The calculations neglect the slight lengthening of the DNA double helix due to intercalation. As is true for linear ds-DNA, entanglement with even one polymer molecule can explain our observed extensions. However, our data do not exclude sc-DNA entanglements with a larger average number of HEC molecules.[42]

At 0.45% HEC, transition to the random coil stretch−contraction cycle occurs for sc-DNA (not shown). Maximum extension along the electric field axis is longer than in 0.16% HEC because of the higher frictional drag forces exerted on the molecule. The transition to steady state takes somewhat longer, as expected in this more viscous medium.

Periodic Behavior. To investigate the periodicity of the 40 kbp sc-DNA extension-contraction cycle, we use the autocorrelation function defined by eq 1. Figure 6 shows A_{vv} and A_{RR}, V_{cm}, and R_l averaged autocorrelation functions, respectively, for 40 kbp sc-DNA in 0.16% HEC and 0.05% HEC. The autocorrelation functions are averaged over 7−10 molecules. The 40 kbp sc-DNA shows significant periodicity in its extension−contraction cycle, especially in slightly entangled HEC. A highly periodic extension−contraction cycle in entangled HEC may be a result of regular, strong entanglements with HEC occurring within the sc-DNA. Of course, the averaged autocorrelation functions are averages over different topoisomers. Inadequate sampling of the population of sc-DNA may account for the less periodic oscillations in 0.05% HEC. A_{vv} and A_{RR} oscillate with the same frequency, as expected. To define the characteristic oscillation time of the extension-contraction cycle, τ_0, we use the first maximum in A_{vv} for 40 kbp sc-DNA. The extension−contraction cycle is about 20% longer in 0.16% HEC than in 0.05% HEC solution. As expected, the characteristic oscillation time does not scale directly with the 3-fold increase in solution viscosity from 0.05% HEC to 0.16% HEC.

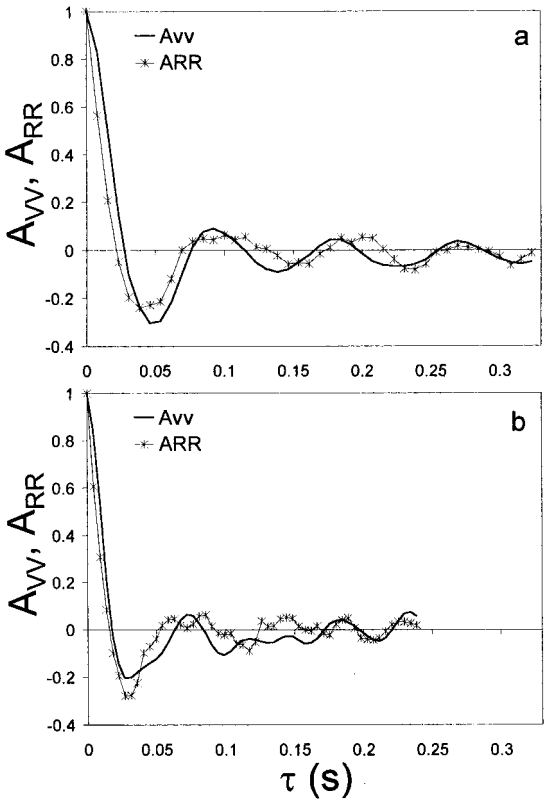

Figure 6. Average V_{cm} autocorrelation functions, A_{vv}, and R_l autocorrelation functions, A_{RR}, for 40 kbp sc-DNA in (a) 0.16% HEC, 1X TBE, and (b) 0.05% HEC, 1X TBE, 100 V/cm. Autocorrelation functions were averaged over 7−10 molecules.

Other points in the autocorrelation plots can also be used to evaluate periodicity. Examples include the first zero crossing, used by Oana and co-workers,[8] and the first minimum. The conclusions reached are independent of the choice of metric.

Figure 7 shows the averaged autocorrelation functions for linear λ ds-DNA in 0.05% HEC and 0.008% HEC. Characteristic oscillation times were defined as the first maximum in A_{RR}. The characteristic oscillation time in 0.05% HEC is only 10% larger than that in 0.008% HEC. The autocorrelation functions show that there is less periodicity in the extension−contraction cycle of linear DNA than in sc-DNA. With linear DNA, A_{vv} and A_{RR} do not oscillate with the same frequency. This is a result of DNA segment density shifting during entanglements with HEC, generating oscillations in V_{cm} not associated with extensions in R_l. Supercoiled DNA A_{vv} and A_{RR} oscillate with the same frequency because plasmid electrophoretic motion is constrained by tightly wound supercoils.

Polymer Entanglements. Supercoiled DNA can adopt various linear and slightly kinked shapes in solution.[18] A perturbing electric field and viscous drag forces cause the sc-DNA to explore a range of tertiary

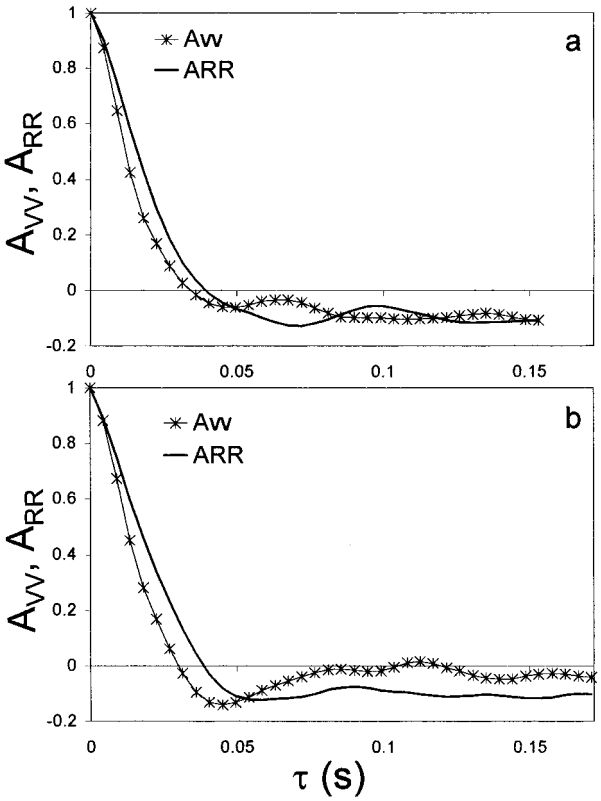

Figure 7. Average V_{cm} autocorrelation functions, A_{VV}, and R_l autocorrelation functions, A_{RR}, for 48.5 kbp linear DNA in (a) 0.05% HEC, 1X TBE, and (b) 0.008% HEC, 1X TBE, 100 V/cm. Autocorrelation functions were averaged over 15−30 molecules.

forms. HEC may collide anywhere along the constantly changing molecule and entangle in any of many kinks and crevices.[19] The resulting transient aggregates may have quite different average shapes.

The stretch-contraction cycle occurs as the sc-DNA reacts to the HEC frictional drag force. Regardless of where collision initially occurs, in the electric field the response of the dynamic structure is to move the HEC to the trailing end of the supercoiled molecule. There are possible explanations for this effect. The movement of supercoils along the molecule forces the double helices involved in the supercoiling to slide by one another.[19] Alternatively, the polymer may work itself down through the supercoils. Of course, a combination of the two mechanisms could be used to adjust HEC polymer position along the sc-DNA. As HEC disengages from the sc-DNA, the elastic restoring force causes the center of mass to spring forward, resulting in collapse of the extended state. The behavior is similar to that of an elastic rod with a large spring constant.

Figure 8 shows the average R_l extension−contraction profiles for both 40 kbp sc-DNA and 48.5 kbp linear DNA. Figure 8a indicates that the extension−contraction cycle of the 40 kbp sc-DNA is symmetric. In 0.16% HEC, the extension−contraction cycle persists for a longer time because of the slightly longer extension of the molecule and, in particular, because of the higher viscosity of the polymer medium. The symmetry of the average R_l profile indicates that the kinetics of extension and collapse are similar for sc-DNA.

In contrast, Figure 8b shows the extension−contraction cycle for 48.5 kbp linear DNA to be very asymmetric. The long extension period leading to the maximum in R_l is a result of long-lived U or J shapes. After release from entangling polymers, the collapse back to the random coil is rapid. This same asymmetric profile has been observed for linear ds-DNA in gels.[8] Figure 8c illustrates the average R_l profile for both 40 kbp sc-DNA and linear λ ds-DNA in 0.05% HEC.

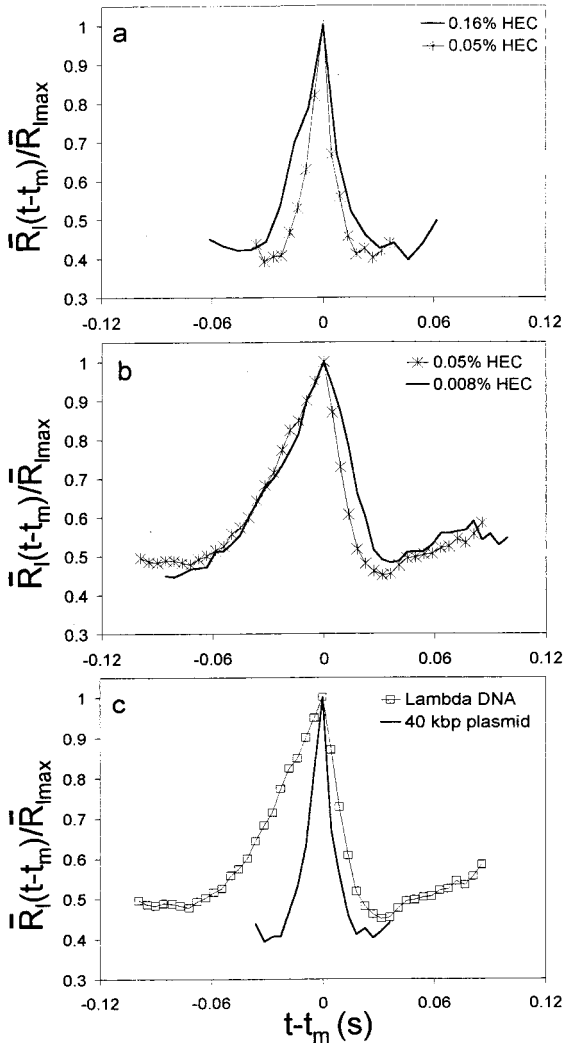

Figure 8. Average time evolution of the R_l profile for 40 kbp sc-DNA and 48.5 kbp linear DNA: (a) 40 kbp sc-DNA in 0.16% HEC and 0.05% HEC, 1X TBE, 100 V/cm; (b) 48.5 kbp linear DNA in 0.05% HEC and 0.008% HEC, 1X TBE, 100 V/cm; (c) R_l profile comparison for 40 kbp sc-DNA and 48.5 kbp linear DNA in 0.05% HEC. R_l profiles were averaged over 10−20 maxima in R_l and normalized with respect to $\bar{R}_{l_{max}}$.

Discussion

Broad, asymmetric bands are observed for linear DNA 5 kbp or greater during capillary electrophoresis in dilute linear polymers.[43] This band-broadening mechanism has been termed dispersion.[37,38] Mobility dispersion of linear ds-DNA during electrophoresis results from a distribution in DNA−polymer disentanglement lifetimes. Mobility dispersion has been shown to increase with electric field strength, gel or polymer concentration, and DNA size.[37−40] Field inversion capillary electrophoresis in dilute linear polymers has been shown to increase the periodicity of linear ds-DNA motions, decreasing mobility dispersion.[44]

Because the sc-plasmid broad bands observed during dilute polymer capillary electrophoresis[24,25] are a result of a distribution of topoisomers rather than mobility

dispersion, it is unclear whether the bandwidth of an individual topoisomer is comparable to that of a linear fragment of the same size in base pairs. However, sc-DNA electrophoretic dynamics are completely different from those of linear ds-DNA. Supercoiled DNA electrophoretic motions are more periodic than linear DNA of the same size in base pairs (Figures 6 and 7). The rates of sc-DNA extension and contraction with polymer capture and release are very similar (Figure 8), unlike linear ds-DNA.

The very periodic oscillatory behavior of sc-DNA electrophoretic dynamics suggests less mobility dispersion than linear ds-DNA of the same size in base pairs.[44] There is evidence in support of our arguments,[30] but more experiments are necessary to completely resolve individual topoisomers and compare the bandwidths quantitatively to that of linear ds-DNA. At this time, mobility dispersion of sc-plasmid topoisomers in dilute polymer solutions has not been explored.

Collision-based descriptions of electrophoretic migration have predicted the effects of the concentration of the separation medium and electric field strength better than classical mechanisms based on such concepts as sieving and reptation. Refinements are possible as our experimental and theoretical understanding of the details of DNA electrophoretic dynamics increases.

Large plasmids in extended external fields may serve as easily visualized models of elastic rod polymer behavior. Experiments that exploit flow-induced extension or other kinds of mechanical extension can now be expected to yield important new information on polymer solution dynamics with important consequences not only for biosciences which depend heavily on electrophoresis but also for all fields which rely on the physics of polymer solutions.

Acknowledgment. We gratefully acknowledge support from the National Institutes of Health and a sponsored research agreement from Matrigen Inc. We thank Elizabeth Smiley and Suqing Wang for the preparation of the plasmids. Additional thanks to Dr. Steve Parus for help generating the electrophoresis control voltage program. J.J.S. was supported by the University of Michigan Biotechnology Training Program. R.W.H. was supported by a summer fellowship from the ACS Division of Analytical Chemistry. H.O. was supported by the Research Fellowship of the Japan Society for Promotion of Science for Young Scientists.

References and Notes

(1) Schwartz, D. C.; Koval, M. *Nature* **1989,** *338*, 520−522.
(2) Smith, S. B.; Aldridge, P. K.; Callis, J. B. *Science* **1989**, *243*, 203−206.
(3) Song, L.; Maestre, M. F. *J. Biomol. Struct. Dyn.* **1991**, *9*, 525−536.
(4) Shi, X.; Hammond, R. W.; Morris, M. D. *Anal. Chem.* **1995**, *67*, 1132−1138.
(5) Shi, X.; Hammond, R. W.; Morris, M. D. *Anal. Chem.* **1995**, *67*, 3219−3222.
(6) Carlsson, C.; Larsson, A.; Jonsson, M.; Nordén, B. *J. Am. Chem. Soc.* **1995**, *117*, 3871−3872.
(7) Hammond, R. W.; Shi, X.; Morris, M. D. *J. Microcolumn Sep.* **1996**, *8*, 201−210.
(8) Oana, H.; Masubuchi, Y.; Matsumoto, M.; Doi, M.; Matsuzawa, Y.; Yoshikawa, K. *Macromolecules* **1994**, *27*, 6061−6067.
(9) Doi, M.; Edwards, S. F. *Theory of Polymer Dynamics*; Oxford University Press: New York, 1986; pp 289−323.
(10) Perkins, T. T.; Smith, D. E.; Larson, R. G.; Chu, S. *Science* **1995**, *268*, 83−87.
(11) Perkins, T. T.; Smith, D. E.; Chu, S. *Science* **1994**, *264*, 819−822.
(12) Perkins, T. T.; Quake, S. R.; Smith, D. E.; Chu, S. *Science* **1994**, *264*, 822−826.
(13) Smith, S. B.; Finzi, L.; Bustamante, C. *Science* **1992**, *258*, 1122−1126.
(14) Fishman, D. M.; Patterson, G. D. *Biopolymers* **1996**, *38*, 535−552.
(15) Langowski, J.; Giesen, U. *Biophys. Chem.* **1989**, *34*, 9−18.
(16) Sambrook, J.; Fritsch, E. F.; Maniatis, T. *Molecular Cloning, A Laboratory Manual*; Cold Spring Harbor Laboratory: Cold Spring Harbor, NY, 1989; pp 1.2−1.110.
(17) Vologodskii, A. *Topology and Physics of Circular DNA*; CRC Press: Boca Raton, FL, 1992; pp 31−47.
(18) Schlick, T. *Curr. Opin. Struct. Biol.* **1995**, *5*, 245−262.
(19) Marko, J. F. *Physica A* **1997**, *244*, 263−277.
(20) Samori, B.; Siligardi, G.; Quagliariello, C.; Weisenhorn, A. L.; Vesenka, J.; Bustamante, C. J. *Proc. Natl. Acad. Sci. U.S.A.* **1993**, *90*, 3598−3601.
(21) Henderson, E. *Nucleic Acids Res.* **1991**, *20*, 445−447.
(22) Barron, A. E.; Soane, D. S.; Blanch, H. W. *J. Chromatogr.* **1993**, *652*, 3−16.
(23) Barron, A. E.; Blanch, H. W.; Soane, D. S. *Electrophoresis* **1994**, *15*, 597−615.
(24) Hammond, R. W.; Oana, H.; Schwinefus, J. J.; Bonadio, J.; Morris, M. D. *Anal. Chem.* **1997**, *69*, 1192−1196.
(25) Oana, H.; Hammond, R. W.; Schwinefus, J. J.; Wang, S. C.; Doi, M.; Morris, M. D. *Anal. Chem.* **1998**, *70*, 574−579.
(26) Pulleyblank, D. E.; Shure, M.; Tang, D.; Vinograd, J.; Vosberg, H.-P. *Proc. Nat. Acad. Sci. U.S.A.* **1975**, *72*, 4280−4284.
(27) Depew, R. E.; Wang, J. C. *Proc. Natl. Acad. Sci. U.S.A.* **1975**, *72*, 4275−4279.
(28) Goldstein, E.; Drlica, K. *Proc. Natl. Acad. Sci. U.S.A.* **1984**, *81*, 4046−4050.
(29) Rill, R. L.; Locke, B. R.; Liu, Y.; Van Winkle, D. H. *Proc. Natl. Acad. Sci. U.S.A.* **1998**, *95*, 1534−1539.
(30) Mao, D. T.; Levin, J. D.; Yu, L.; Lautamo, R. M. A *J. Chromatogr. B* **1998**, *714*, 21−27.
(31) Smith, S. B.; Bendich, A. J. *Biopolymers* **1990**, *29*, 1167−1173.
(32) Mitnik, L.; Heller, C.; Prost, J.; Viovy, J. L. *Science* **1995**, *267*, 219−222.
(33) Hjerten, S. J. *J. Chromatogr.* **1985**, *347*, 191−198.
(34) Savitzky, A.; Golay, M. J. E. *Anal. Chem.* **1964**, *36*, 1627−1639.
(35) Press: W. H.; Teukolsky, S. A.; Vetterling, W. T.; Flannery, B. P. *Numerical Recipes in C*; 2nd ed.; Cambridge University Press: Cambridge, U.K., 1992; p 545.
(36) Ueda, M.; Oana, H.; Baba, Y.; Doi, M.; Yoshikawa, K. *Biophys. Chem.* **1998**, *71*, 113−123.
(37) Weiss, G. H.; Sokoloff, H.; Zakharov, S. F.; Chrambach, A. *Electrophoresis* **1996**, *17*, 1325−1332.
(38) Yarmola, E.; Calabrese, P. P.; Chrambach, A.; Weiss, G. H. *J. Phys. Chem. B* **1997**, *101*, 2381−2387.
(39) Schwinefus, J. J.; Morris, M. D. *Analyst* **1998**, *123*, 1481−1485.
(40) Gibson, T. J.; Sepaniak, M. J. *J. Chromatogr. B* **1997**, *695*, 103−111.
(41) Strick, T. R.; Allemand, J.-F.; Bensimon, D.; Bensimon, A.; Croquette, V. *Science* **1996**, *271*, 1835−1837.
(42) Hubert, S. J.; Slater, G. W.; Viovy, J.-L. *Macromolecules* **1996**, *29*, 1006−1009.
(43) Kim, Y.; Morris, M. D. *Anal. Chem.* **1994**, *66*, 3081−3085.
(44) Schwinefus, J. J.; Morris, M. D. *Macromolecules* **1999**, *32*, 3678−3684.

MA990129X